Overview of direct reaction theory

Filomena Nunes
Michigan State University

FRIB-TA Topical Program Bound state to continuum, East Lansing, June 2018

Direct reactions: examples

Textbook definition:

short timescale, only a few relevant degrees of freedom, retains information from initial state

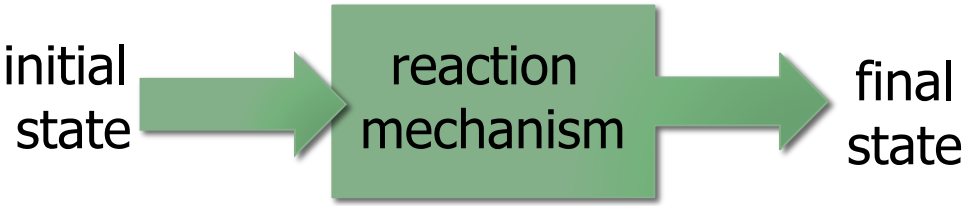

Examples:

- Elastic scattering
- Inelastic nuclear excitation
- Coulomb excitation
- Transfer reactions
- Knockout reactions
- Breakup
- Charge exchange reactions

Charge exchange to IAS,
Danielewicz, NPA 958 (2017) 147.

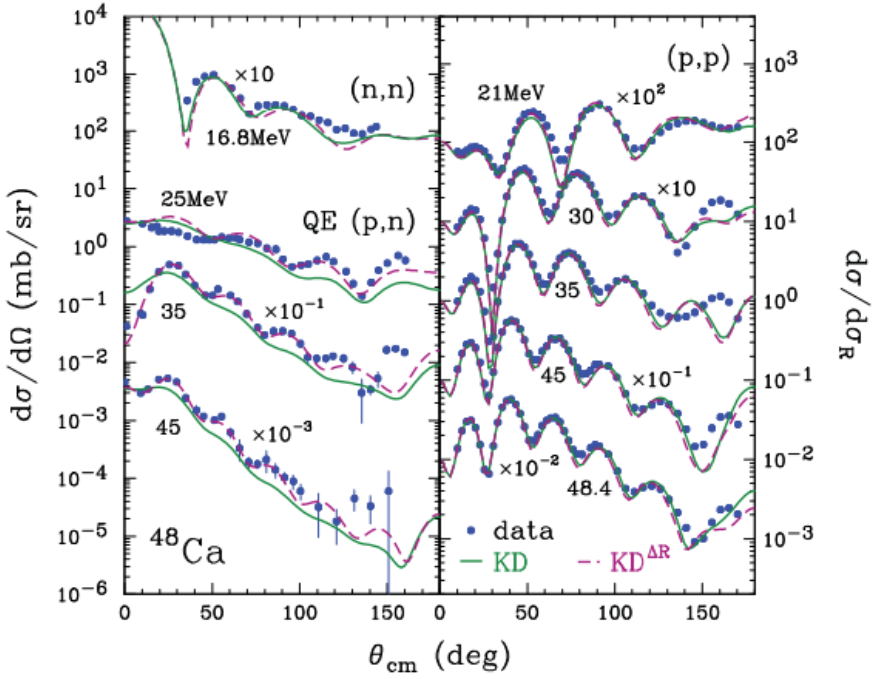

Direct reactions: general theory

- Observables are cross sections (angular distributions, energy distributions, polarization observables, etc)
- Cross sections are proportional to $|T|^2$

$$T^{exact} = < \chi_f^{(-)} \mid V \mid \Psi_i^{(+)} >$$

exact

Two traditional approaches:

Coordinate space (solve for wfn)

$$H\Psi = E\Psi, \quad \Psi(R \to \infty) = (F + TH^+)$$

Momentum space (typically solve for tmatrix)

$$T = V + VG_0T, \quad G_0 = (E - H_0)^{-1}$$

$$T = V + VG_0T$$

Direct reactions: Born series

- Iterate Lippman Schwinger Equation $\Psi = \phi + G_0 V \Psi$

$$\Psi = \phi + G_0 V \phi + G_0 V G_0 V \phi + G_0 V G_0 V G_0 V \phi + ...$$

$$T = -\frac{2\mu}{\hbar^2 k}(< \phi|V|\phi > + < \phi|V G_0 V|\phi > + < \phi|V G_0 V G_0 V|\phi > + ...)$$

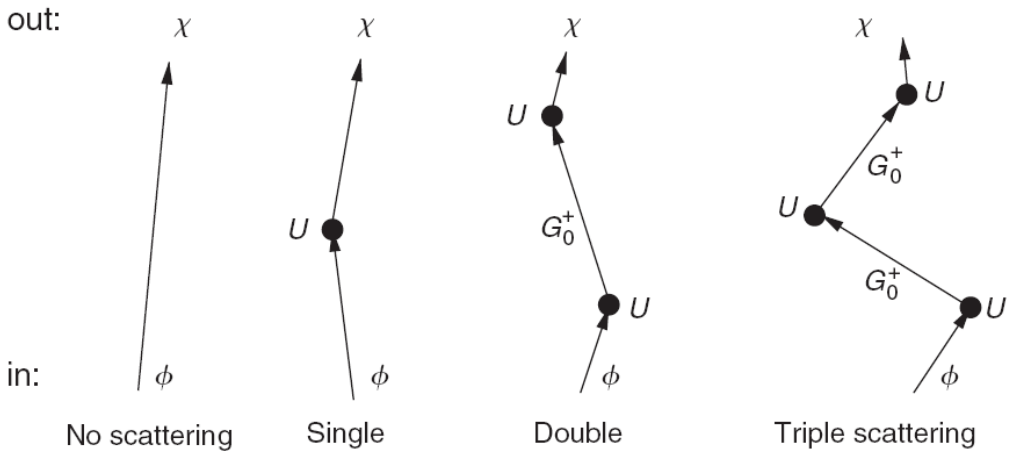

Perturbative approaches based on Born series

- Make a choice on what part of the interaction is left out of the propagator

$$\Psi = \chi_1 + G_1 V_2 \Psi, \quad G_1 = (E - (T + V_1))^{-1}$$

- Iterate to retain only first (and second) term of the Born series

(V_2 should be weaker than V_1)

Direct reactions: a few d.o.f.

- Identify relevant channels and reduce many-body problem

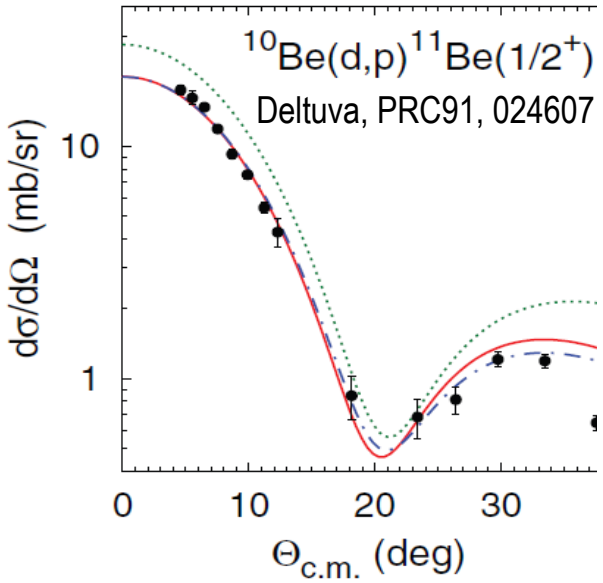

Typical reductions:

- two-body, three-body, four-body, etc
- single-particle or cluster degrees of freedom
- collective degrees of freedom (deformations, etc)

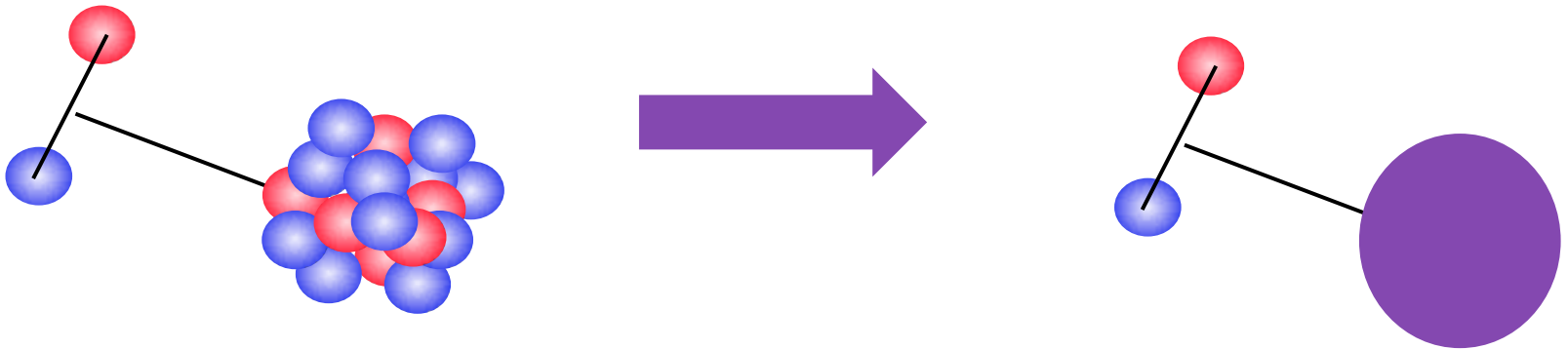

Direct reactions: general remarks

1. Few nucleon reactions to direct reactions with nuclei:

   Coulomb force much stronger and exact treatment needed!

2. Reactions not equal to resonances:

   Non-resonant continuum critical for describing dynamics!

3. Direct reactions are sensitive to peripheral behaviour:

   Asymptotics needs to be correct. Bound state bases don't work!

4. Reactions are extremely sensitive to thresholds:

   Q-value sets the overall magnitude for the process!

Direct reactions: typical inputs

1. Q-values and separation energies: thresholds
2. Optical potentials
3. Overlap functions (one nucleon, two nucleon, alpha, etc)
4. Transition densities

Outline

1. Faddeev approach
2. Continuum discretized coupled channel method
3. Adiabatic methods
4. Eikonal methods
5. Time dependent methods
6. 4-body extensions
7. Including core excitation
8. Uncertainties

Faddeev Approach

3-body Hamiltonian:

$$H_{3b} = \hat{T} + V_{vc} + V_{vt} + V_{ct}$$

$$\Psi = \sum_{n=1} \Psi^{(n)}(\mathbf{r}_n, \mathbf{R}_n)$$

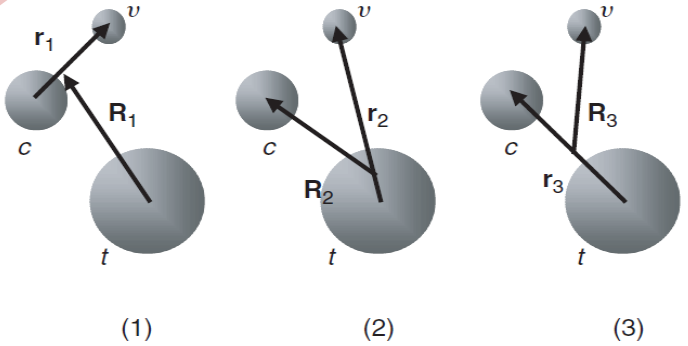

Faddeev Equations:

$$(E - T_1 - V_{vc})\Psi^{(1)} = V_{vc}(\Psi^{(2)} + \Psi^{(3)})$$

$$(E - T_2 - V_{vt})\Psi^{(2)} = V_{vt}(\Psi^{(3)} + \Psi^{(1)})$$

$$(E - T_3 - V_{tc})\Psi^{(3)} = V_{tc}(\Psi^{(1)} + \Psi^{(2)})$$

Watch out for Linda Hlophe's talk and for Jin Lei's talk

Often written in T-matrix form and in the momentum space (AGS equations)

Transfer components are asymptotically separated:

$$\Psi^{(n)} \to \sum_p \phi_p^{(n)}(\mathbf{r}_n)\psi_p^{(n)}(\mathbf{R}_n) + \text{breakup; when } R_n \to \infty$$

Continuum Discretized Coupled Channel Method

- Pick one Jacobi coordinate set for basis expansion

$$[H_{3b} - E]\Psi^{(1)}(\mathbf{r}_1, \mathbf{R}_1) = 0$$

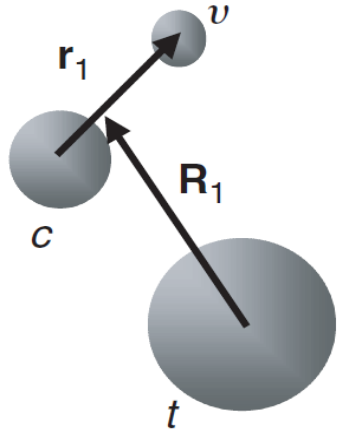

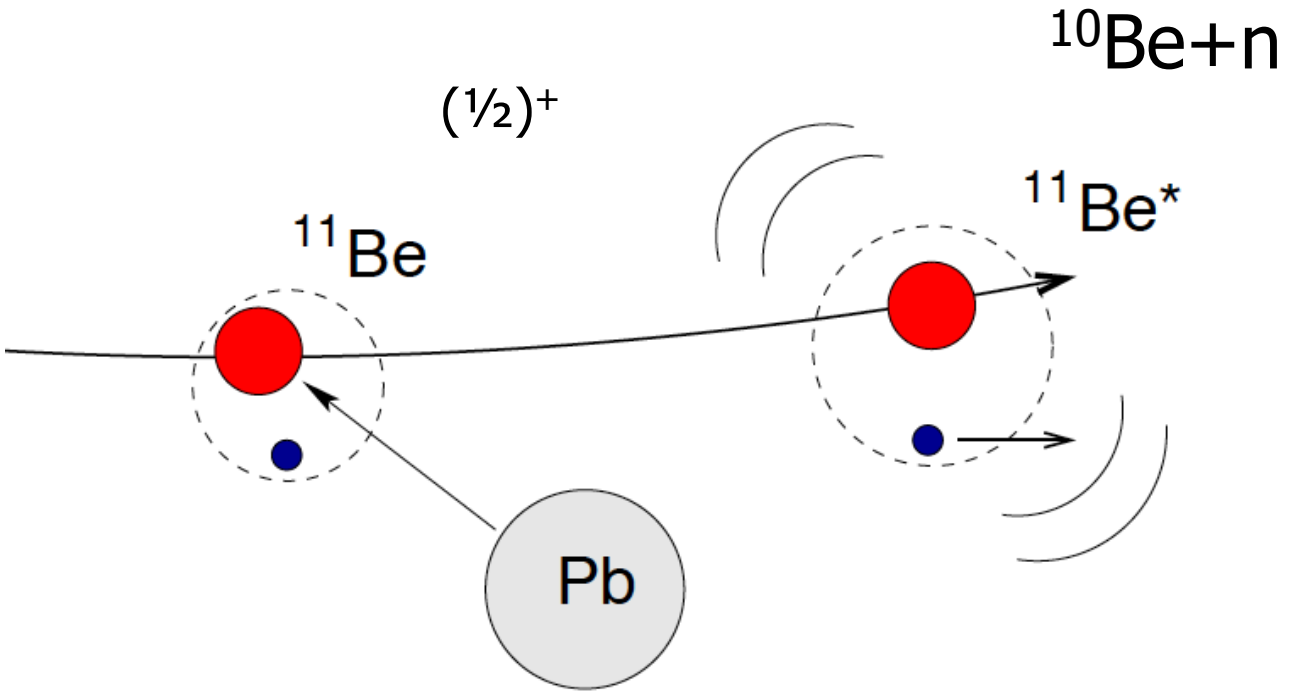

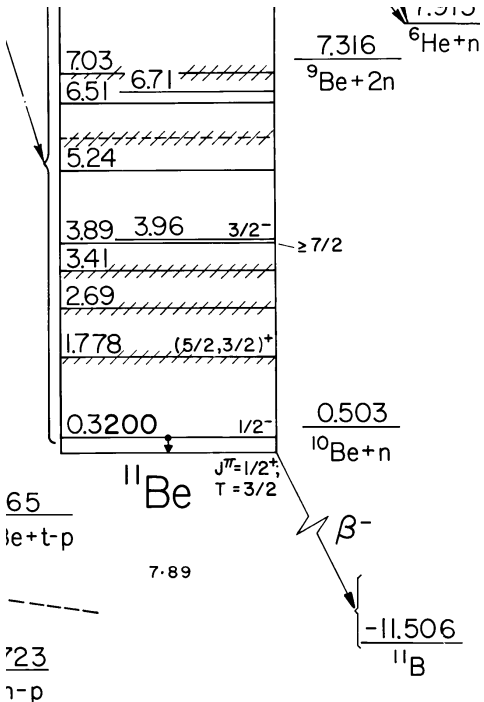

Continuum Discretized Coupled Channel Method

- Pick one Jacobi coordinate set for basis expansion

$$[H_{3b} - E]\Psi^{(1)}(\mathbf{r}_1, \mathbf{R}_1) = 0$$

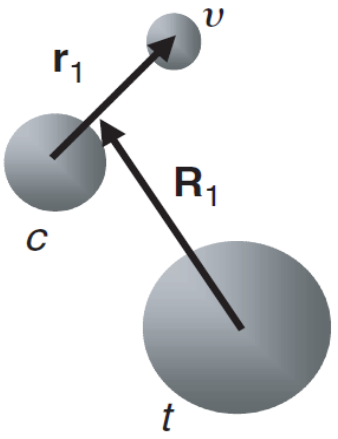

Expand wfn in eigenstates of projectile's internal Hamiltonian:

$$\Psi^{(1)}_{\mathbf{K}_0}(\mathbf{r}_1, \mathbf{R}_1) = \sum_{p=1}^{n_b} \phi_p(\mathbf{r}_1)\psi_p(\mathbf{R}_1) + \int \mathrm{d}\mathbf{k}\, \phi_{\mathbf{k}}(\mathbf{r}_1)\psi^{\mathbf{k}}_{\mathbf{K}}(\mathbf{R}_1)$$

Energy conservation

$$E_{\mathrm{cm}} + \epsilon_0 = E = \frac{\hbar^2 k^2}{2\mu_{vc}} + \frac{\hbar^2 K^2}{2\mu_{(vc)t}}$$

Continuum States as basis

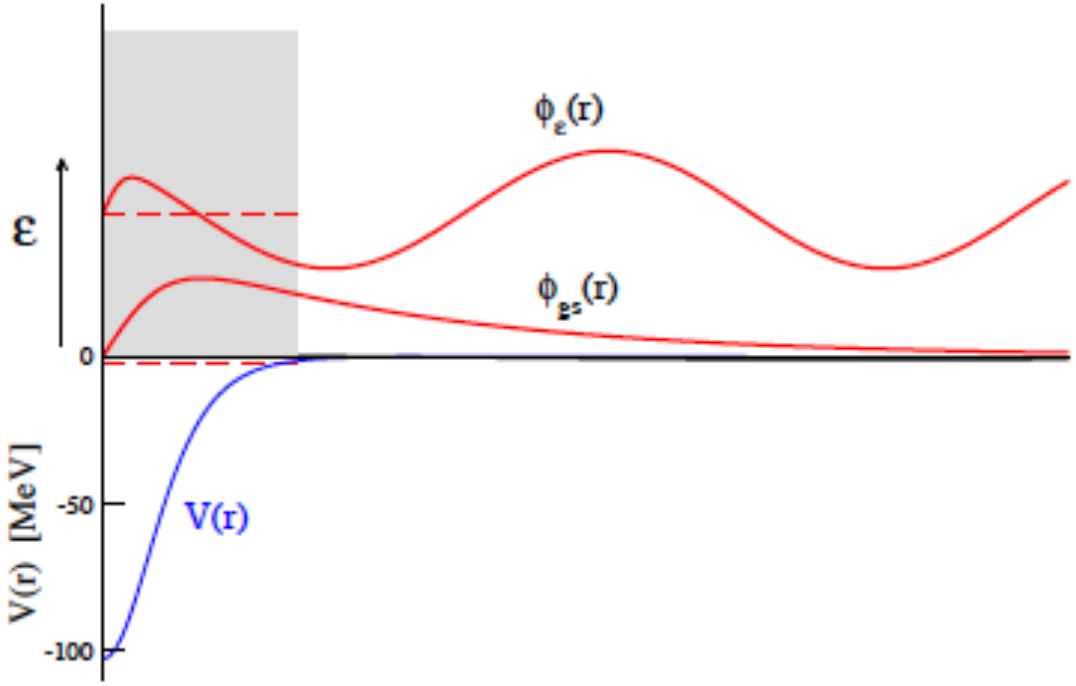

Scattering state

Bound state

- Energy/momentum: a continuous variable
  - infinite number of energy states!!
- Continuum states oscillate and never die off for large R
  - non-normalizable!!

Bad problems ☹

Continuum Bins as basis

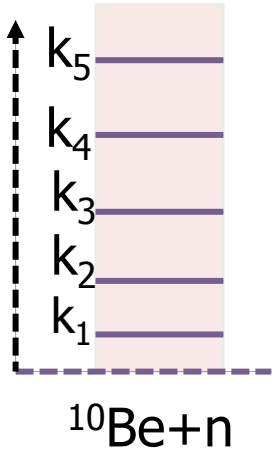

average method

$$\tilde{u}_p(r) = \sqrt{\frac{2}{\pi N_p}} \int_{k_{p-1}}^{k_p} g_p(k) u_k(r)\, \mathrm{d}k$$

analytic form if potential is zero and l=0:

$$\tilde{u}_p(r) \propto \sin(k_p r) \frac{\sin((k_p - k_{p-1})r)}{r}$$

- Discrete number of bins
- Normalizable – square integrable
- For non-overlaping continuum intervals, continuum bins are orthogonal

Can form a good basis!

Continuum Discretized Coupled Channel Method

CDCC 3-body wavefunction:

$$\Psi^{\mathrm{CDCC}}(\mathbf{r},\mathbf{R}) = \sum_{p=0}^{N} \tilde{\phi}_p(\mathbf{r})\psi_p(\mathbf{R})$$

$$p = \{lsjI_cI_p;(k_{p-1},k_p)\}$$

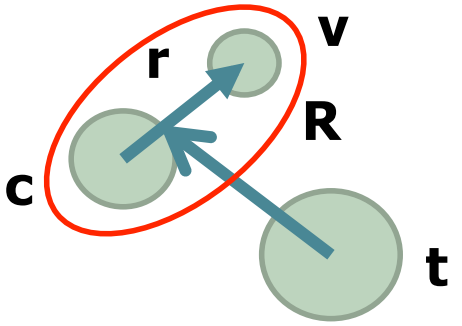

Coupled channel equations: $(H_{3\mathrm{b}} - E)\Psi^{\mathrm{CDCC}}(\mathbf{r},\mathbf{R}) = 0$

$$[\hat{T}_R + V_{pp}(R) - E_p]\psi_p(\mathbf{R}) + \sum_{p'\neq p} V_{pp'}(R)\psi_{p'}(\mathbf{R}) = 0$$

Coupling potentials: $V_{pp'}(R) = \langle\tilde{\phi}_p(r)|U_{vt}+U_{ct}|\tilde{\phi}_{p'}(r)\rangle$

Energies: $E_p = E-\tilde{\epsilon}_p$ $\qquad \tilde{\epsilon}_p = \langle\tilde{\phi}_p(\mathbf{r})|H_{\mathrm{int}}|\tilde{\phi}_p(\mathbf{r})\rangle$

CDCC: there are many applications

CDCC + set of single particle parameters
- extract ANC from χ^2 minimum
- error from $\varepsilon=\chi_{min}^2+1$

Yao, JPG33 (2006) 1

$$ANC = 1.32 \pm 0.07 \text{ fm}^{-1/2}$$

Summers et al., PRC78(2009)069908

^{208}Pb(^{15}C,^{14}C+n)^{208}Pb@68 MeV/u

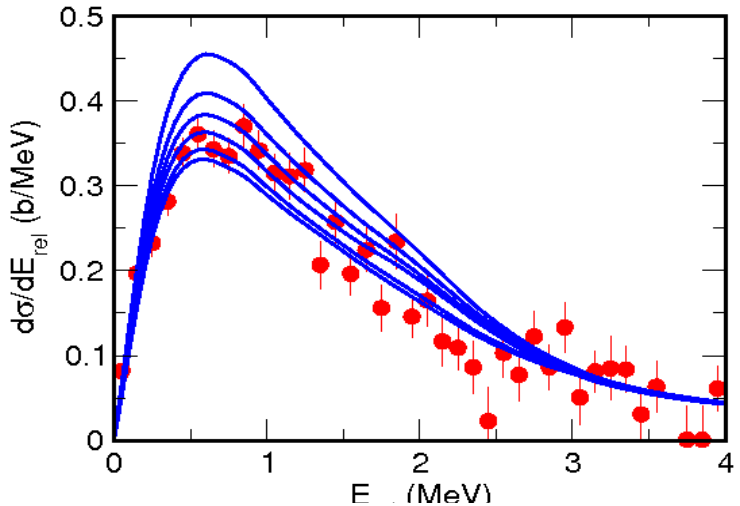

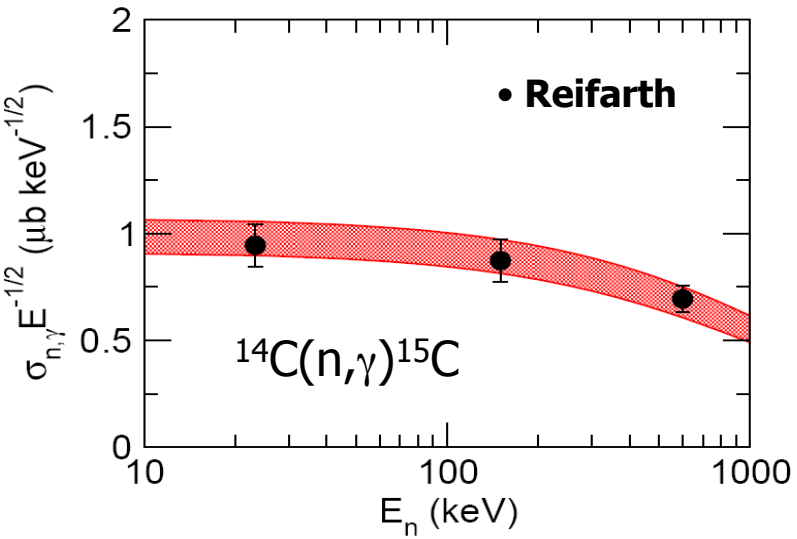

Reifarth, PRC77,015804 (2008)

Nakamura et al, NPA722(2003)301c

Faddeev versus CDCC for breakup

angular distributions

energy distribution

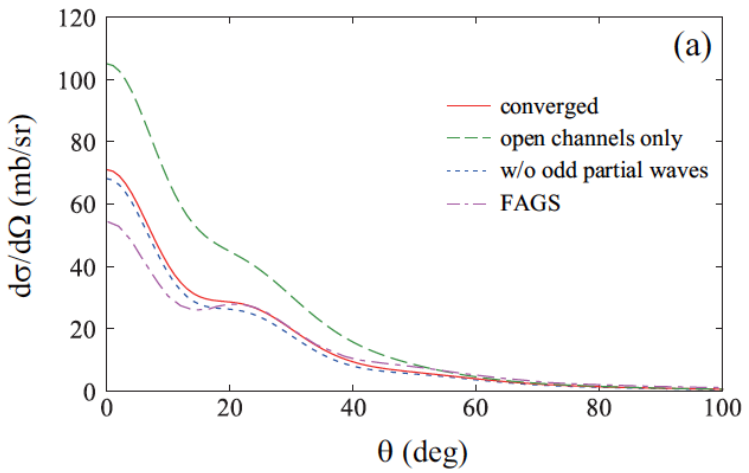

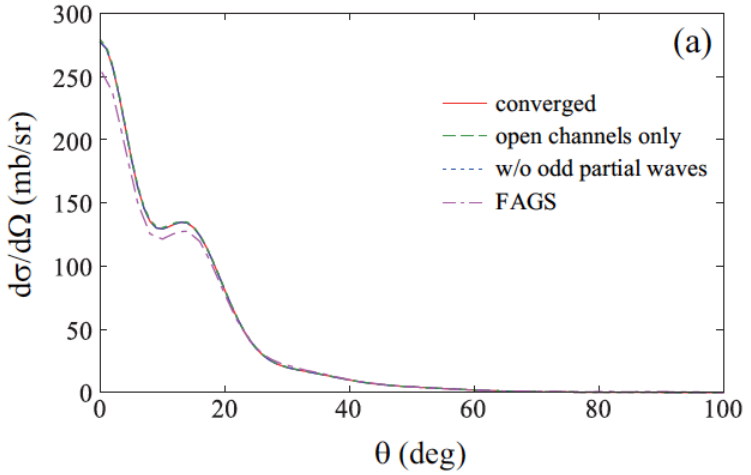

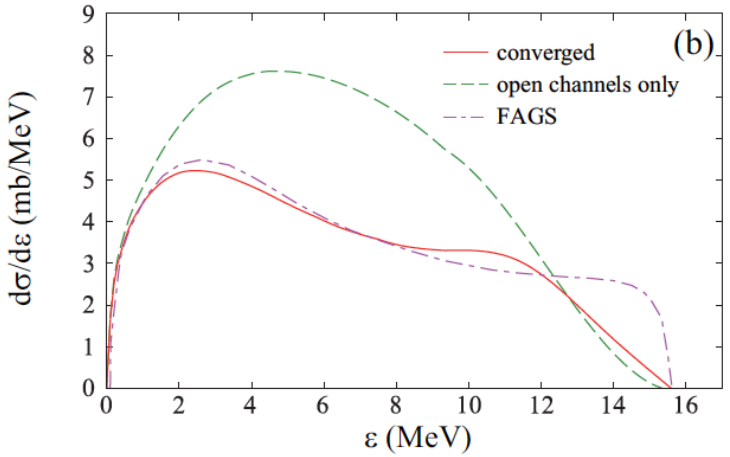

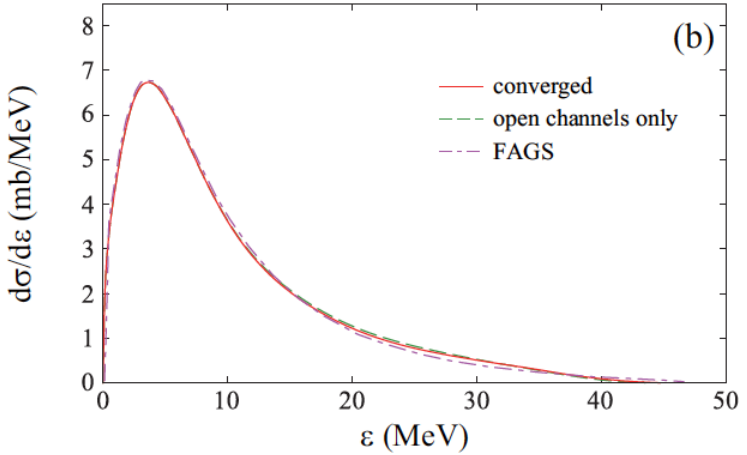

^{10}Be(d,pn) ^{10}Be @ 21 MeV

^{12}C(d,pn) ^{12}C @ 56 MeV

Importance of closed channels!

Ogata and Yoshida, PRC94, 051603(2016)

Adiabatic methods: general

- Based on the separation of fast variable R and slow variable r
- Reductions of the CDCC equations assuming excitation energy of projectile can be neglected

$$\Psi = \phi_0(\mathbf{r})\chi_0(\mathbf{R}) + \sum_{i>0}\phi_i(\mathbf{r})\chi_i(\mathbf{R})$$

$$[\hat{T}_R + \epsilon_0 + U_{ct} + U_{vt} - E]\phi_0(\mathbf{r})\chi_0(\mathbf{R}) + \sum_{i>0}[\hat{T}_R + \epsilon_i + U_{ct} + U_{vt} - E]\phi_i(\mathbf{r})\chi_i(\mathbf{R}) = 0$$

$$|\epsilon_i - \epsilon_0| \ll E$$

$$(\hat{T}_R + U_{ct} + U_{vt} - (E - \epsilon_0))\Psi^{\mathrm{ad}}(\mathbf{r},\mathbf{R}) = 0$$

$$\Psi(\mathbf{r},\mathbf{R}) \approx \Psi^{\mathrm{ad}}(\mathbf{r},\mathbf{R}) = \phi_0(\mathbf{r})\chi_0^{\mathrm{ad}}(\mathbf{R}) + \sum_{i>0}\phi_i(\mathbf{r})\chi_i^{\mathrm{ad}}(\mathbf{R})$$

Adiabatic method for A(d,p)B reactions

- The exact T-matrix simplifies for intermediate and heavy targets

$$T_{dp}^{exact} =< \phi_{nA}\ \chi_{pB}^{(-)}\ |V_{np} + U_{pA} - U_{pB}|\ \Psi_d^{(+)}(\vec{r}_{np}, \vec{R}_d) >$$

$$T_{dp}^{exact} =< \phi_{nA}\ \chi_{pB}^{(-)}\ |V_{np}|\ \Psi_d^{(+)}(\vec{r}_{np}, \vec{R}_d) >$$

Only need the exact deuteron incident wave in the range of Vnp!

$$T_{dp}^{ad} \approx< \phi_{nA}\ \chi_{pB}^{(-)}\ |V_{np}|\ \phi_d\ \chi_{ad}^{(+)}(\vec{r}_{np}, \vec{R}_d) >$$

$$U_{JS}(R) = U_{nA}(\vec{R}) + U_{pA}(\vec{R})$$

Adiabatic plus zero range

[Johnson and Soper, Phys. Rev. C 1, 976(1970)]

$$U_{ij}(\vec{R}) = -\langle\phi_i|V_{np}(U_{nA} + U_{pA}|\phi_j\rangle$$

Weinberg basis

[Johnson and Tandy, NPA 235, 56(1974)]

Adiabatic methods: applications

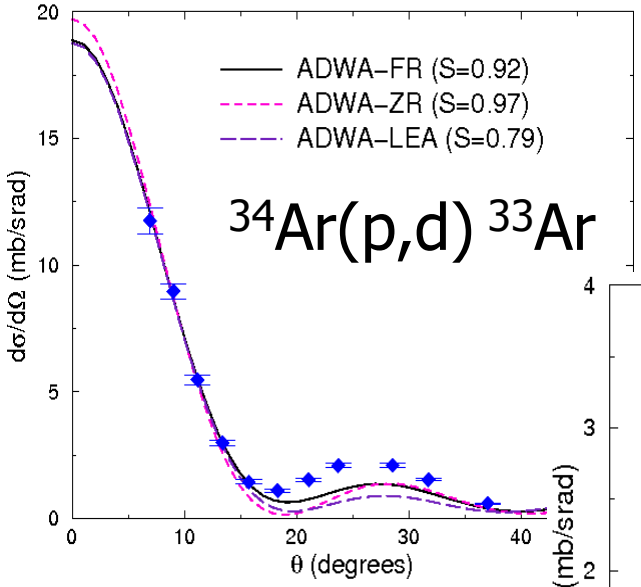

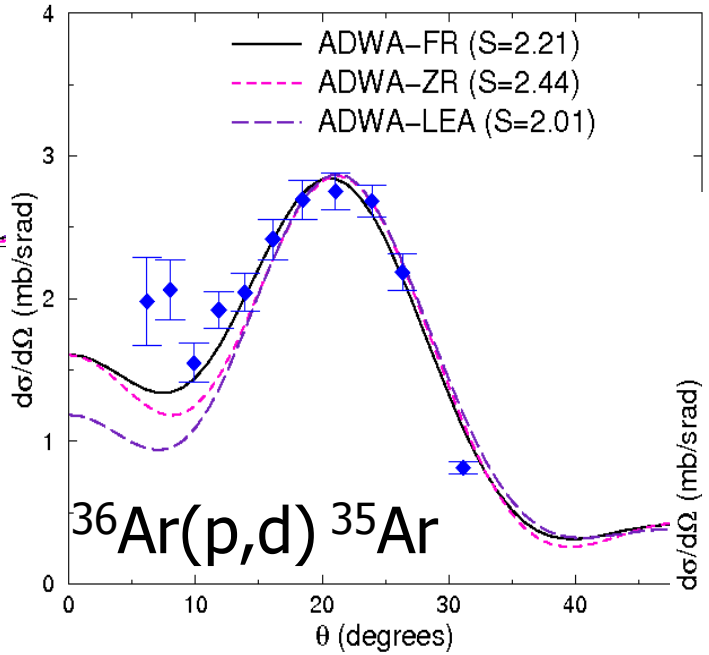

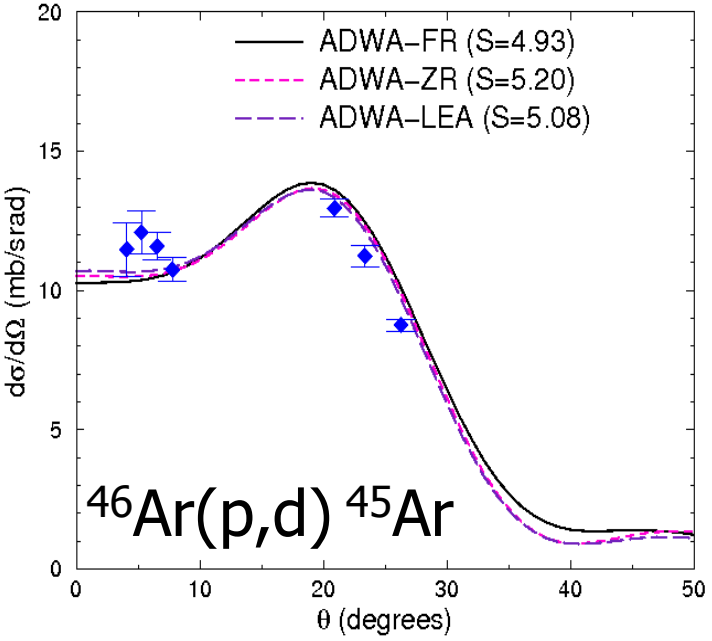

[FN, Deltuva, Hong, Phys. Rev. C 83, 034610 (2011)]

Adiabatic versus CDCC

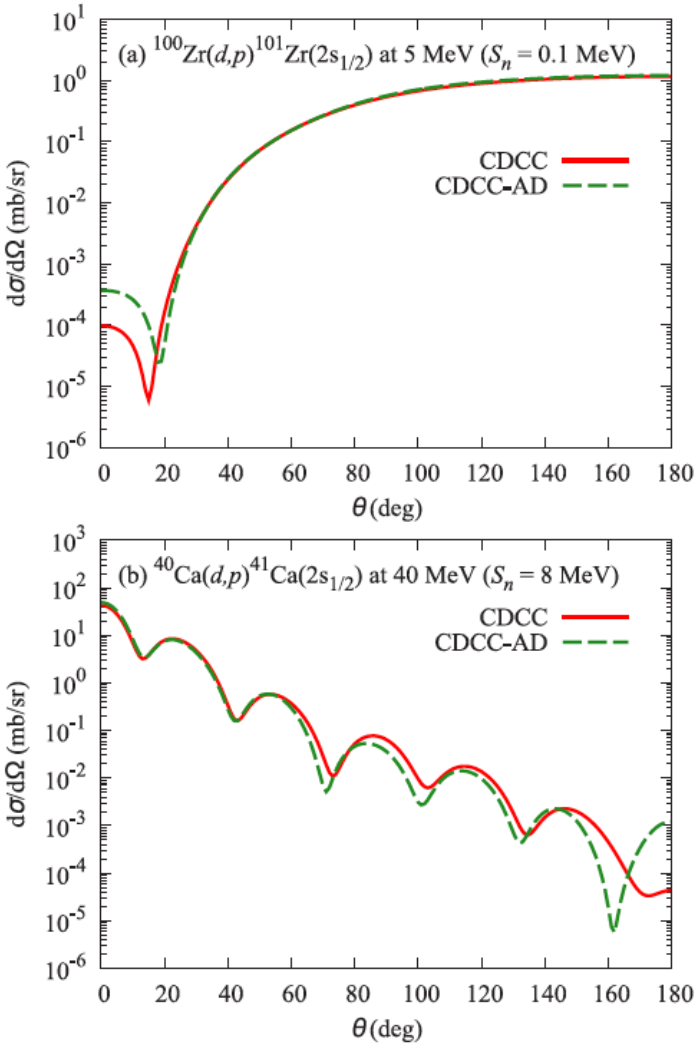

FIG. 2. Angular distributions of the (d,p) cross sections calculated with CDCC (solid lines) and CDCC-AD (dashed lines) for (a) ^{100}Zr$(d,p)^{101}$Zr$(2s_{1/2})$ at $E_d = 5$ MeV with $S_n = 0.1$ MeV and (b) ^{40}Ca$(d,p)^{41}$Ca$(2s_{1/2})$ at $E_d = 40$ MeV with $S_n = 8$ MeV.

TABLE II. Adiabatic factor S_{AD}. The superscripts $*1$, $*2$, and $*3$ indicate the cases in which the AD approximation does not work. See the text for details.

$\ell_f = 0$

Target	Energy (S_n = 0.1 MeV)				Energy (S_n = 8 MeV)			
	5	10	20	40	5	10	20	40
^{20}Ne	0.71^{*3}	0.89	1.32	1.25	0.90	0.93	0.88	0.74
^{40}Ca	1.08^{*3}	1.21	2.01^{*2}	1.44^{*2}	0.78	0.77	0.78	0.87
^{100}Zr	0.96	1.11	1.83^{*2}	1.67^{*2}	0.87^{*1}	0.87	0.68	1.10
^{200}Hg	1.00	0.94	1.21	1.29	1.06^{*1}	0.88	0.66	1.24

$\ell_f = 1$

Target	Energy (S_n = 0.1 MeV)				Energy (S_n = 8 MeV)			
	5	10	20	40	5	10	20	40
^{20}Ne	0.94	1.00	0.99	0.92	0.84	0.83	0.83	0.91
^{40}Ca	0.94	0.80	0.87	1.15	0.81^{*1}	0.80	0.93	0.85
^{100}Zr	0.96	0.90	0.74	2.00^{*2}	0.96	0.80	0.85	1.02
^{200}Hg	1.00	0.93	1.06	1.56^{*2}	0.94^{*1}	0.75^{*1}	0.74	0.92

$\ell_f = 2$

[Chazono et al., PRC95, 064608 (2017)]

Eikonal methods (semi-classical)

- Straight-line trajectories

$$\Psi(\mathbf{R}) = e^{ikz}\phi(\mathbf{b}, z) = e^{i(kz+\chi(\mathbf{b},z))}$$

Eikonal phases – phase accumulated through the trajectory

$$\chi(\mathbf{b}, z) = -\frac{1}{\hbar v_p}\int_{-\infty}^{z} V(\mathbf{b}, z')\mathrm{d}z'$$

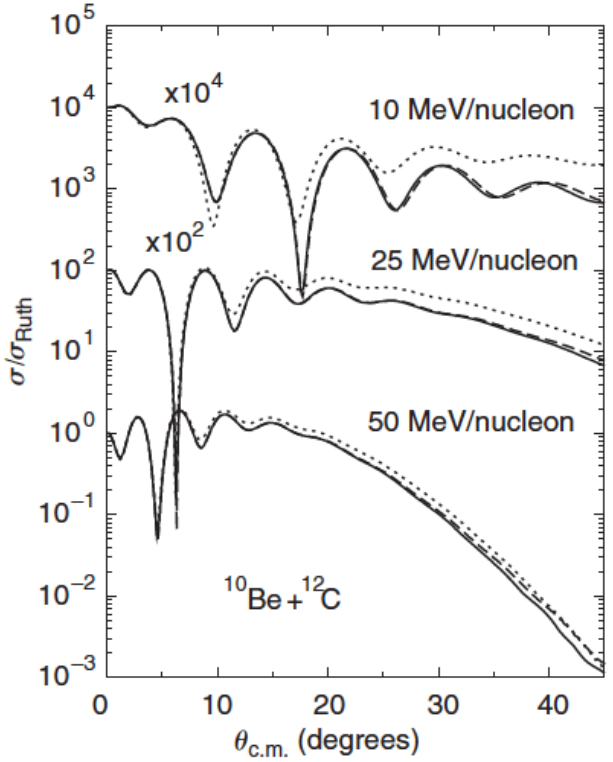

J. M. Brooke, J. S. Al-Khalili and J. A. Tostevin

Eikonal theory for composite projectiles

$$\chi(\mathbf{b}-\mathbf{b}_r) \equiv \sum_{j=1}^{n} \chi(\mathbf{b}-\mathbf{b}_{r_j})$$

$$S_i(\mathbf{b}_i) = \mathrm{e}^{\mathrm{i}\chi_i(\mathbf{b}_i)}$$

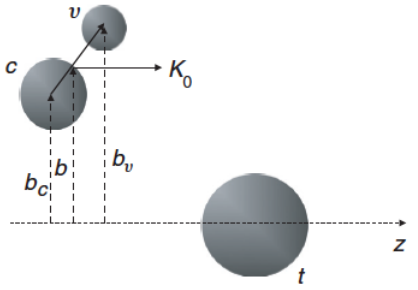

- Glauber formula for composite projectiles (elastic)

$$f_{fi}(\theta) = -\frac{\mathrm{i}K_0}{2\pi}\int \mathrm{d}^2b\,\mathrm{e}^{\mathrm{i}\mathbf{q}\cdot\mathbf{b}}\int\cdots\int \mathrm{d}\mathbf{r}_1\mathrm{d}\mathbf{r}_2\ldots\mathrm{d}\mathbf{r}_{n-1}$$
$$\Phi_f(\mathbf{r}_1,\ldots,\mathbf{r}_{n-1})^*[S_1(\mathbf{b}_1)\ldots S_n(\mathbf{b}_n)-1]\Phi_i(\mathbf{r}_1,\ldots,\mathbf{r}_{n-1})$$

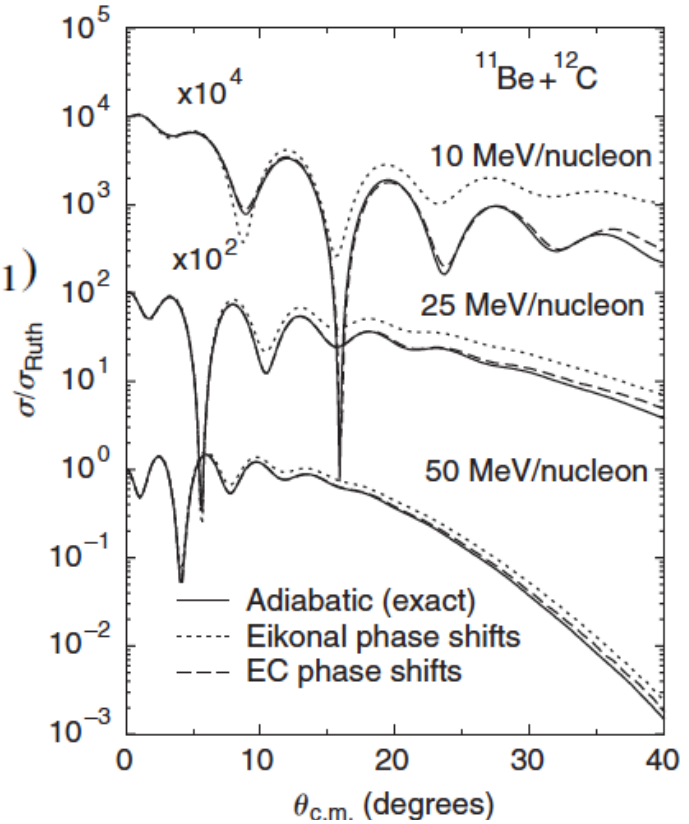

J. M. Brooke, J. S. Al-Khalili and J. A. Tostevin

Eikonal methods applied to knockout

TABLE II. Experimental (σ_{exp}) and calculated (σ_{th}) one-neutron knockout cross sections to the lowest $3/2^+$ and $1/2^+$ states in the mass A_{res} residues. The σ_{th} use the shell-model spectroscopic factors C^2S and their center-of-mass correction, $(A_{proj}/A_{res})^2$, and the calculated eikonal model single-particle cross sections σ_{sp}. All cross sections are in millibarns.

J_f^π	A_{proj}	A_{res}	σ_{sp}	SDPF-MU		SDPF-U		σ_{exp}
				C^2S	σ_{th}	C^2S	σ_{th}	
$3/2_1^+$	36	35	14.2	3.07	46.0	2.61	39.2	29(6)
	38	37	13.8	2.79	40.6	2.19	28.4	19(2)
	40	39	13.3	2.31	32.4	1.69	19.9	14(2)
$1/2_1^+$	36	35	21.1	0.96	21.3	1.00	22.3	13(1)
	38	37	20.7	0.80	17.5	0.97	19.5	10(1)
	40	39	22.7[a]	0.53	12.6	0.72	14.1	

[a]Experimental excitation energy not known. σ_{sp} is calculated with the SDPF-MU shell model energy.

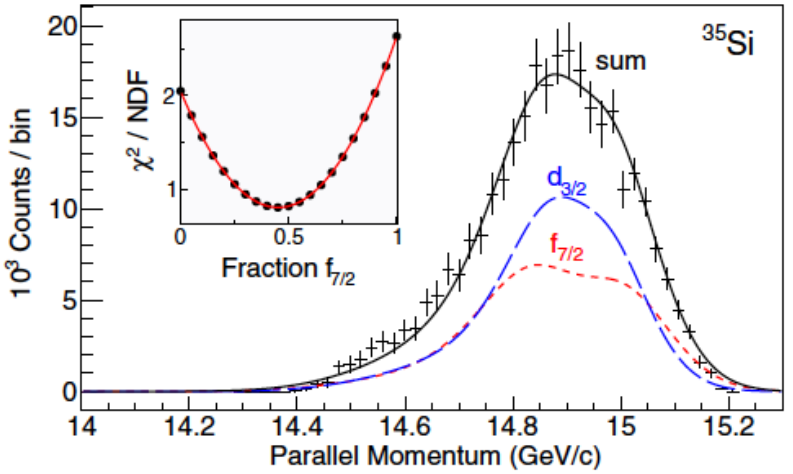

FIG. 2. (Color online) Momentum distribution of the ^{35}Si residues produced in the ground state and any isomers following one neutron knockout from ^{36}Si. The curves show a fit using a linear combination of the calculated distributions for removal from the $f_{7/2}$ and $d_{3/2}$ orbits.

^{9}Be(^{36}Si, ^{35}Si γ) X

[Stroberg et al., PRC91, 041302 (2015)]

Time dependent methods

Our starting point time-dep Schrodinger Eq

$$i\hbar\frac{\partial}{\partial t}\Psi^{\mathrm{TD}}(t,b,\boldsymbol{r}) = [H_0 + V_{PT}(t,\boldsymbol{r})]\,\Psi^{\mathrm{TD}}(t,b,\boldsymbol{r})$$

The interaction is defined by

$$V_{PT}(t,\boldsymbol{r}) = U_{cT}\,[\boldsymbol{R}_c(t)] + U_{fT}[\boldsymbol{R}_f(t)] - \frac{Z_P Z_T e^2}{R(t)}$$

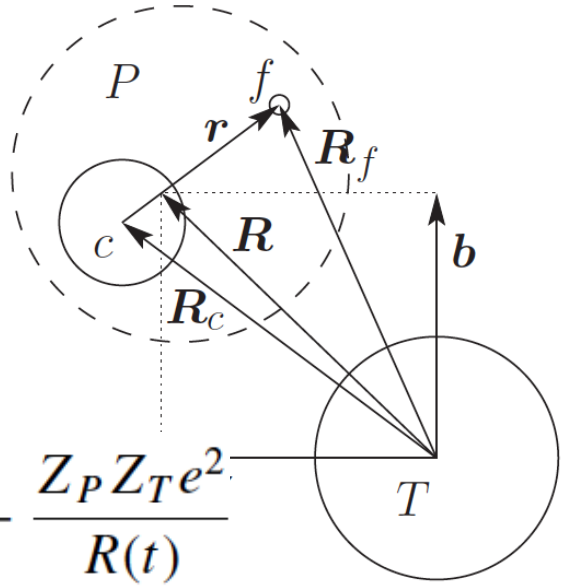

Initial conditions

$$\Psi^{\mathrm{TD}}(t\to-\infty,b,\boldsymbol{r}) = \phi_0(\boldsymbol{r})$$

Probability of breakup is obtained for each trajectory

$$\frac{dP_{\mathrm{bu}}}{dk}(b) \propto \sum_{ljIM}\left|\left\langle\phi_k^{ljIM}\middle|\Psi^{\mathrm{TD}}(t\to+\infty,b)\right\rangle\right|^2$$

Dynamical Eikonal Approx (DEA) Capel, Baye et al.

$$\Psi^{\mathrm{DEA}}(\boldsymbol{R},\boldsymbol{r}) = e^{iK_0Z}\widehat{\Psi}(\boldsymbol{R},\boldsymbol{r})$$

Coulomb Corrections!

$$i\frac{\hbar^2K_0}{\mu_{PT}}\frac{\partial}{\partial Z}\widehat{\Psi}(Z,\boldsymbol{b},\boldsymbol{r}) = [(H_0-E_0)+U_{cT}(\boldsymbol{R}_c)+U_{fT}(\boldsymbol{R}_f)]\widehat{\Psi}(Z,\boldsymbol{b},\boldsymbol{r})$$

Benchmark semi-classical methods

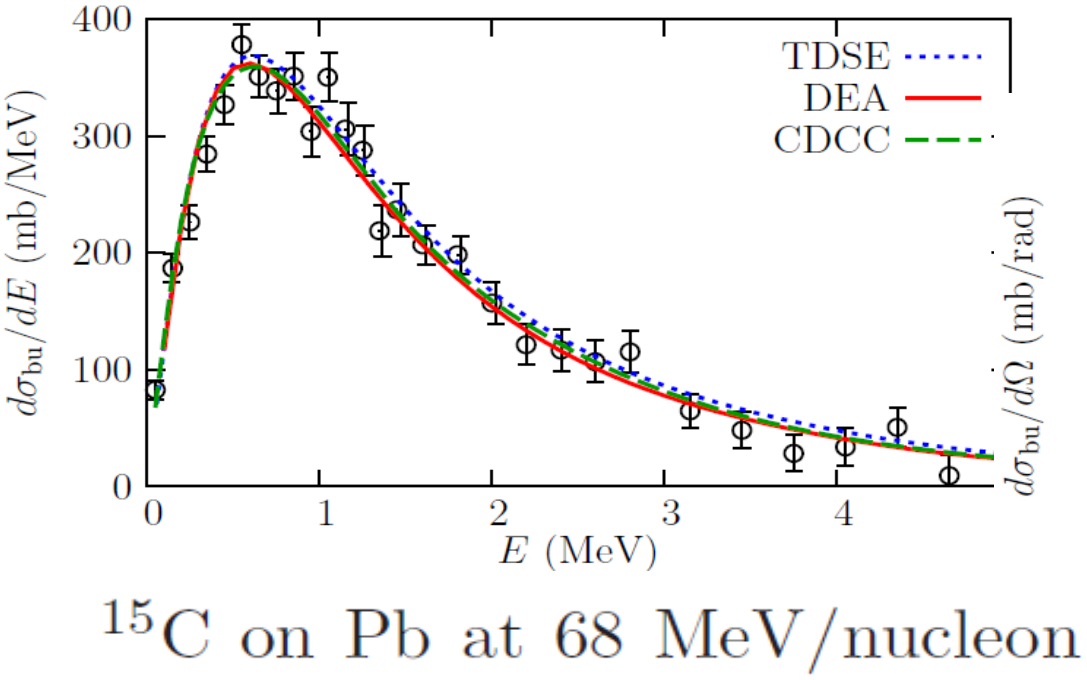

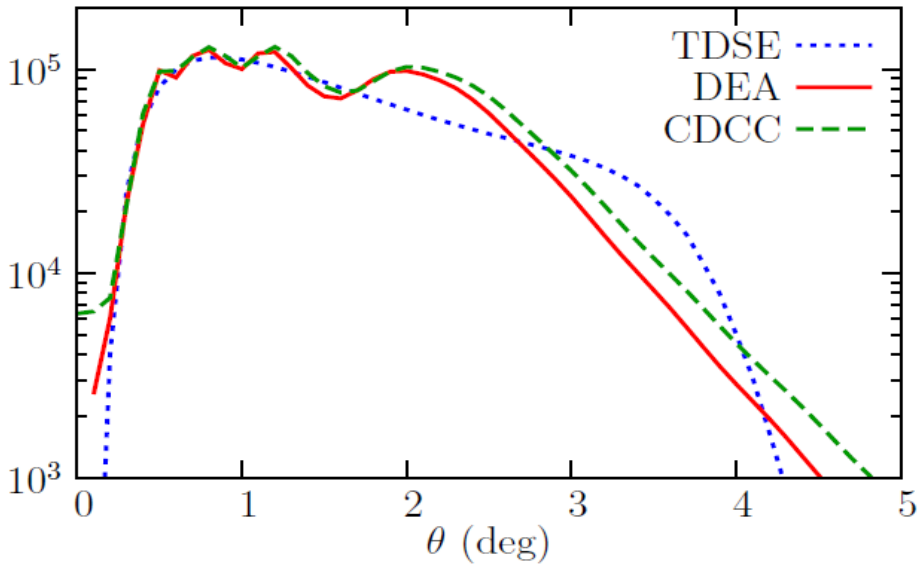

DEA method (with Coulomb correction) does well even below 50 MeV/u

Capel, Esbensen, Nunes, PRC (2011)

Data: Nakamura et al, PRC 79, 035805

DEA application

- Showing the sensitivity to different interactions

$^{12}C(^{11}Be, ^{10}Be+n)\,^{12}C$ E=67 MeV/u

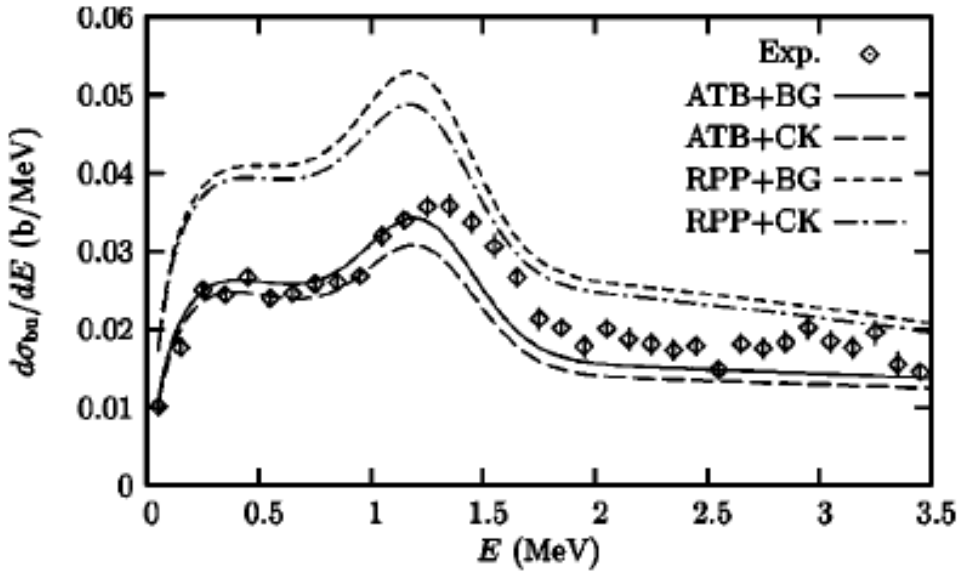

FIG. 4. Theoretical and experimental breakup cross sections as a function of the energy. The four curves correspond to the calculations performed with various combinations of the potentials of Table III convoluted with energy resolution. Experimental data are from Ref. [39].

[Capel et al., PRC70, 064605(2004)]

Outline

1. Faddeev approach
2. Continuum discretized coupled channel method
3. Adiabatic methods
4. Eikonal methods
5. Time dependent methods
6. 4-body extensions
7. Including core excitation
8. Uncertainties

4-body developments

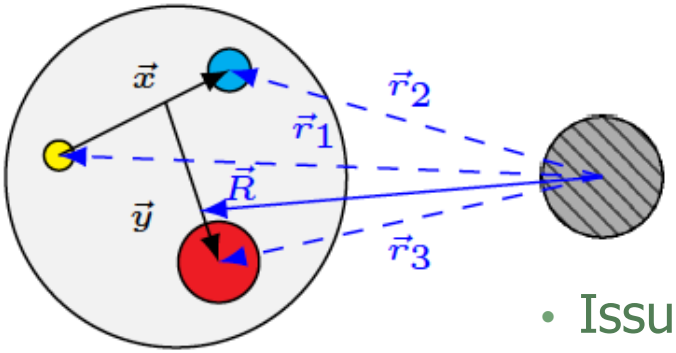

- Issues with convergence
- Stability of the CC eqs

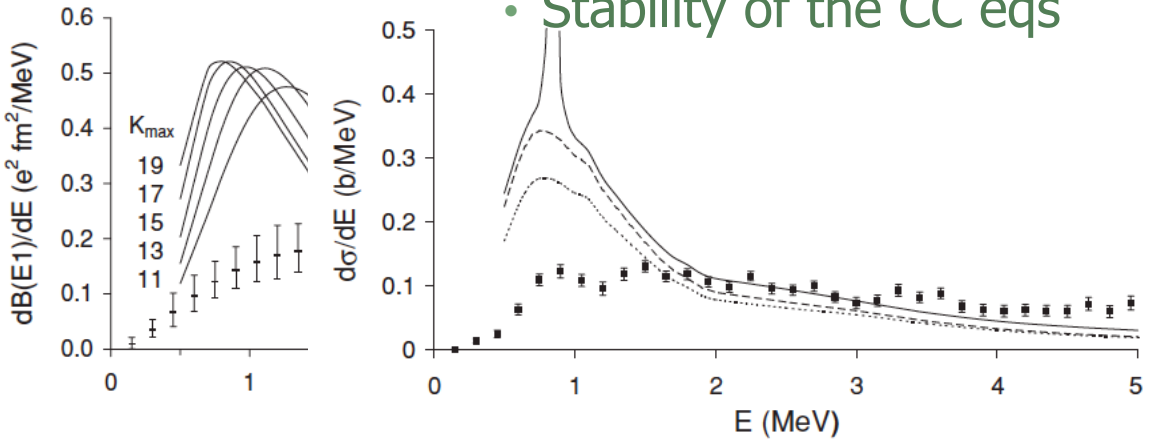

FIG. 2. Convergence respect to the maximum h scattering state: comparis Data from Ref. [23].

FIG. 10. Comparison between the total eikonal cross section (solid line) and 1^- partial cross sections (supersymmetry, dashed line; projection, dotted line) of ^{6}He breakup on ^{208}Pb at 240 MeV/nucleon with the experimental data of Ref. [23].

[Baye et al., PRC79, 024607(2009)]

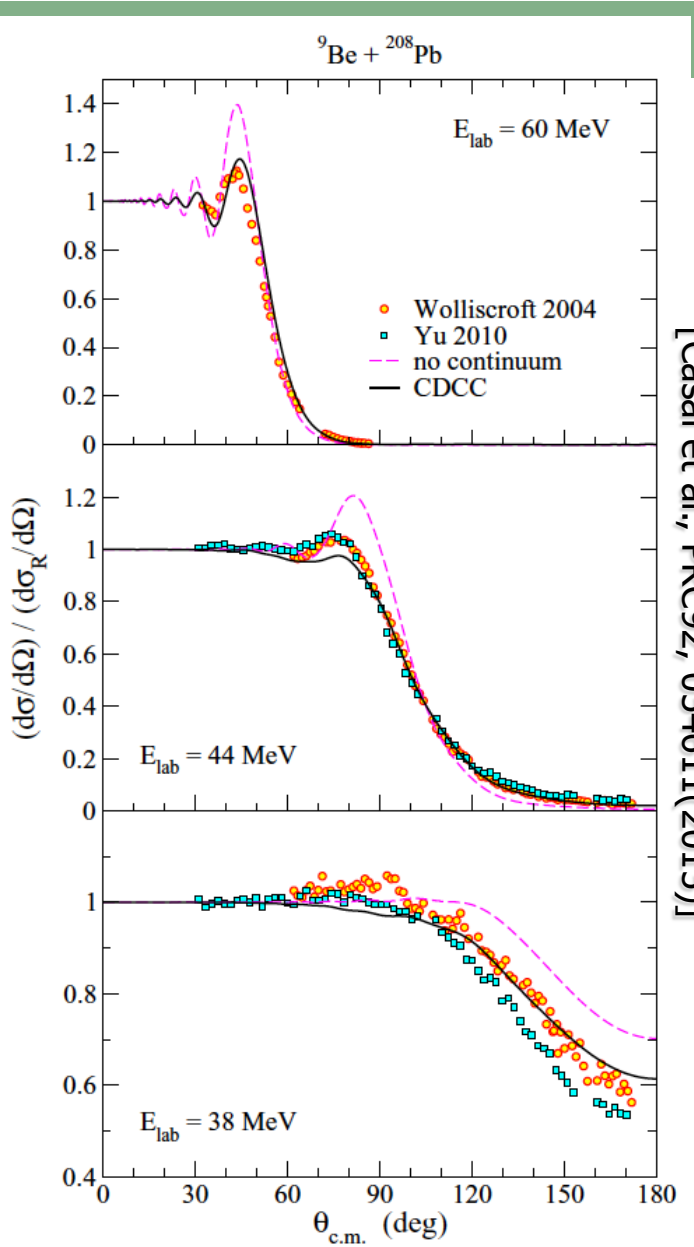

[Casal et al., PRC92, 054611(2015)]

FIG. 7. (Color online) Angular distribution of the elastic cross section relative to Rutherford for the reaction ^{9}Be + ^{208}Pb at E_{lab} = 60, 44, and 38 MeV. Dashed lines correspond to calculations including the ground state only, and solid lines are the full CDCC calculations. The experimental data are shown with circles (Wolliscroft 2004 [23]) and squares (Yu 2010 [24]).

Faddeev with target excitation

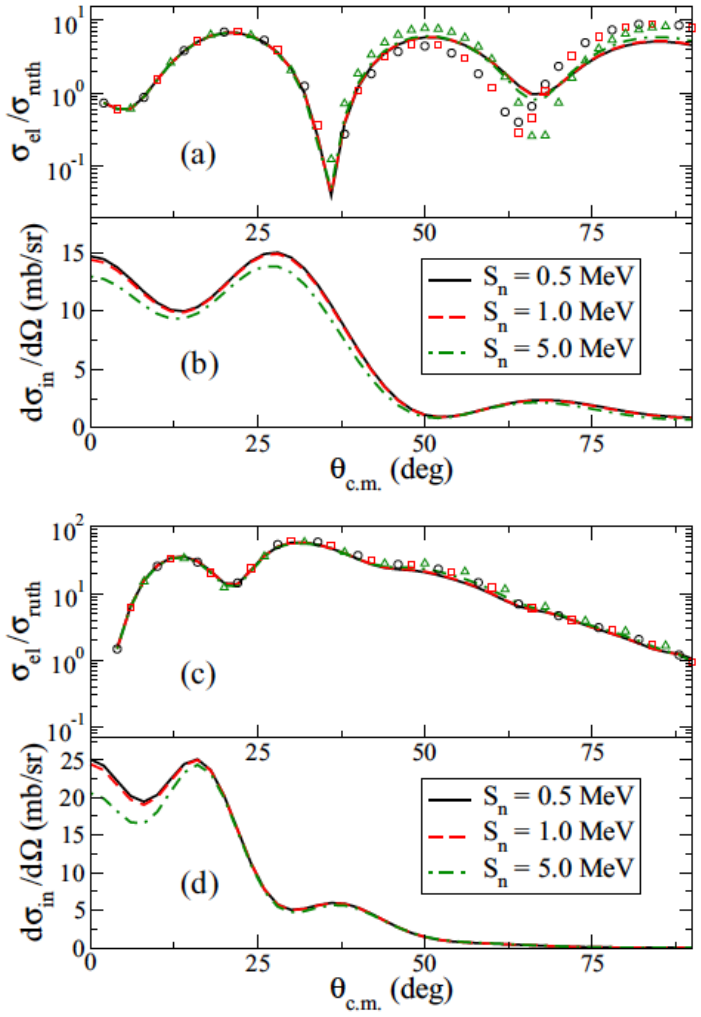

FIG. 2. Angular distributions for ^{10}Be$(d,d)^{10}$Be (ratio to Rutherford) and ^{10}Be$(d,d')^{10}$Be(2^+) at (a), (b) 20 MeV and (c), (d) 80 MeV: Faddeev predictions are obtained for various separation energies of the final nucleus in the (d,p) transfer channel.

- Deuteron induced excitation of ^{10}Be
- Faddeev results incorporating collective model for ^{10}Be

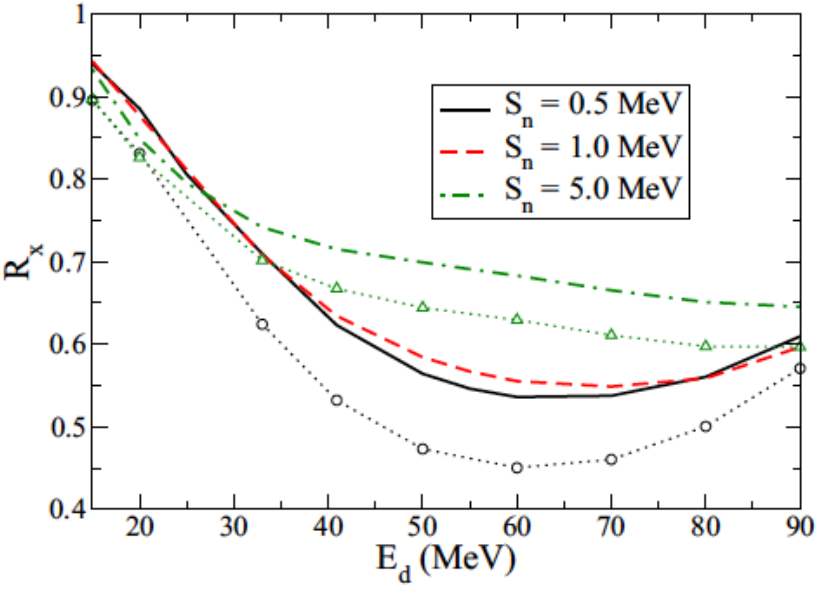

FIG. 3. Spectroscopic factor ratio R_x as a function of beam energy extracted from ^{10}Be$(d,p)^{11}$Be for various separation energies of the final nucleus (more details in the text).

Deltuva, et al. PRC94, 044613(2016)

CDCC with core excitation

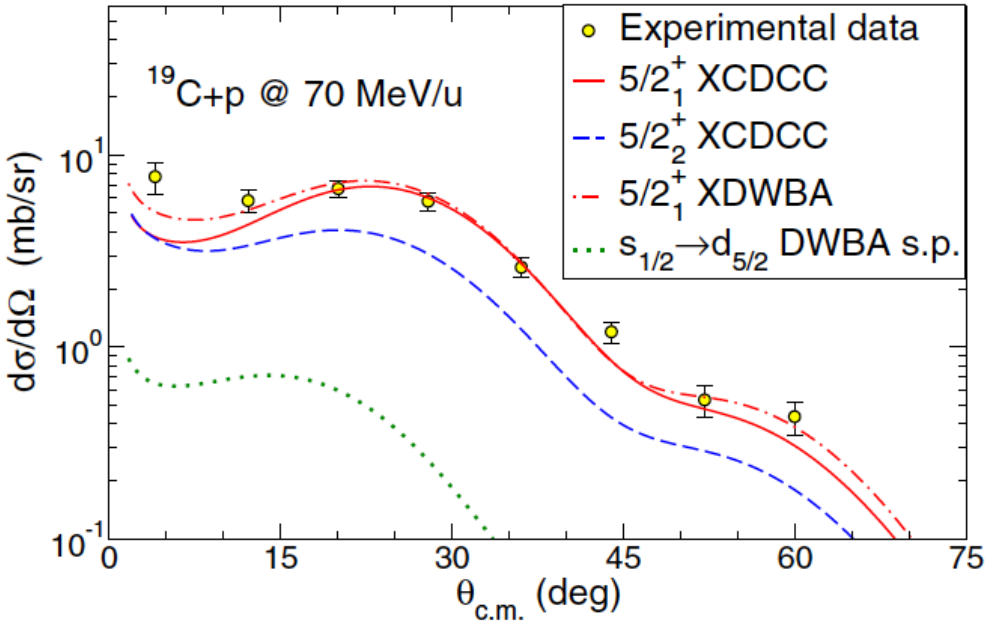

FIG. 2. Angular distribution of the resonant breakup of ^{19}C on protons at 70 MeV/nucleon. The solid red line and the dashed blue line correspond to the XCDCC calculation for the first and the second $5/2^+$ resonance of the P-AMD model [34] respectively. The dotted dashed line corresponds to a XDWBA calculation for the first $5/2^+$ resonance. The dotted line corresponds to an inert-core DWBA calculation where ground state and resonance are considered to be pure $s_{1/2}$ and $d_{5/2}$ states respectively. Experimental data are from Ref. [33].

Our structure calculations, based on a particle-plus-core model of ^{19}C, predict two $5/2^+$ low-lying resonances, but none of them at the energy of the peak observed in [33]. Furthermore, the corresponding angular distributions are both compatible with the shape and magnitude of the experimental one, thus precluding an unambiguous identification of the experimental peak with one or another. This result is understood as a consequence of the similar structure for the two resonances. Both resonances are mainly based on the first 2^+ state of the core. Therefore, it is clearly seen in the present analysis that the dynamic excitation of the core is the main mechanism responsible for the peak observed in the breakup with protons. Moreover, we have shown that the pure valence excitation mechanism, assuming a $2s_{1/2} \rightarrow 1d_{5/2}$ single-particle transition, gives a negligible contribution here. This is the first case where we have identified that the core excitation mechanism dominates overwhelmingly.

Important of closed channels!

Lay et al. PRC94, 021602(2016)

Uncertainties in reactions: (d,p) example

^{90}Zr(d,p)^{90}Zr at 24 MeV

ADWA

$$T^{(d,p)} = \langle \phi_{An} \chi_p | V_{np} | \phi_d \chi_d^{ad} \rangle$$

$$U_{ij}(\vec{R}) = -\langle \phi_i | V_{np} (U_{nA} + U_{pA} | \phi_j \rangle$$

proton elastic data (exit channel)

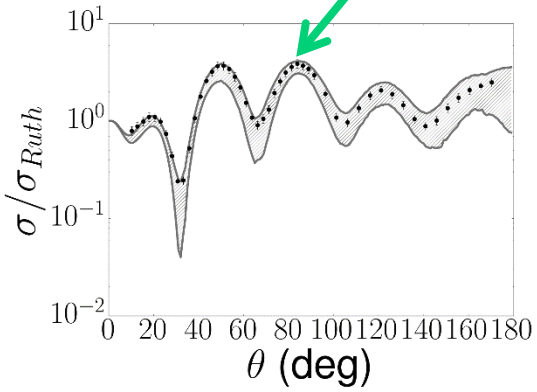

neutron and proton elastic data (entrance channel)

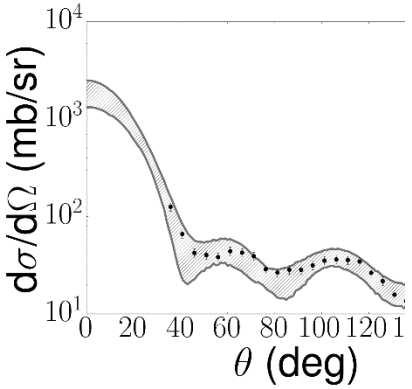

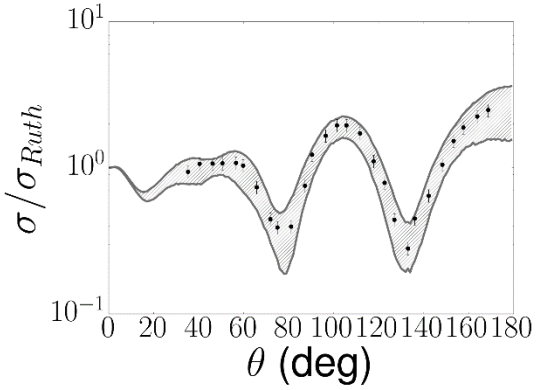

Bayesian: transfer predictions

^{90}Zr(d,p)^{91}Zr at 24 MeV

Lovell and Nunes, PRC (2018) accepted

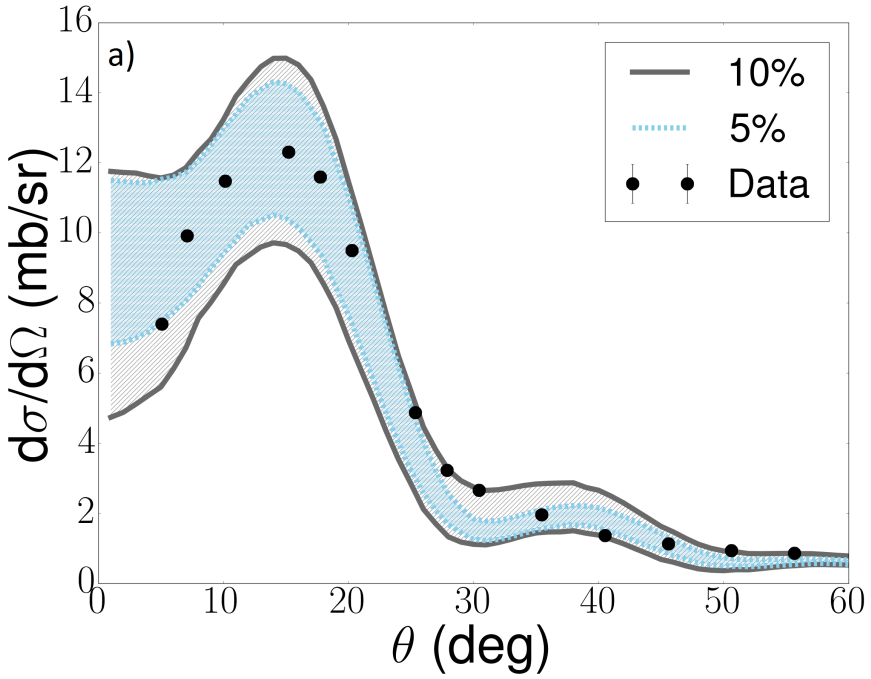

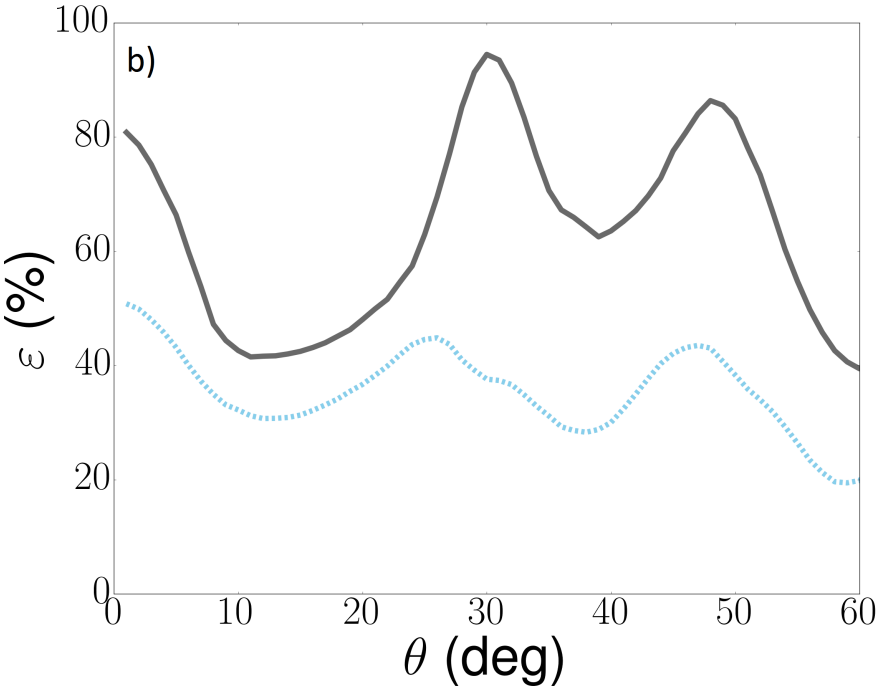

Even with best elastic data, uncertainties on cross sections from the optical potential are too large!

Concluding remarks

- Good understanding of range of validity of the various formulations
- Challenges to incorporate more degrees of freedom:

  4-body, core excitation, etc
- Uncertainty in the inputs
  - We are starting to quantify uncertainties more rigorously and discovering these need to be reduced

- Structure theory can help in providing predictions for some part of the inputs, constraints to others and guidance on how to shape the fitting protocols

Various reaction efforts we are involved with:

Faddeev in Coulomb basis with separable interactions (Hlophe, Lin, CE, AN, FN)

Properties of separable interactions (Quinonez, Hlophe, FN)

Inclusive (d,p) to continuum (Li, Potel, FN)

Uncertainty quantification in reactions (King, Wright, Catacororios, Lovell, FN)

Microscopic optical potential (Rotureau, FN, PD, GH, TP)

Thank you for your attention!

Supported by: NNSA-DOE, NSF

Reaction efforts at MSU

Faddeev in Coulomb basis with separable interactions (Hlophe, Lin, CE, AN, FN)

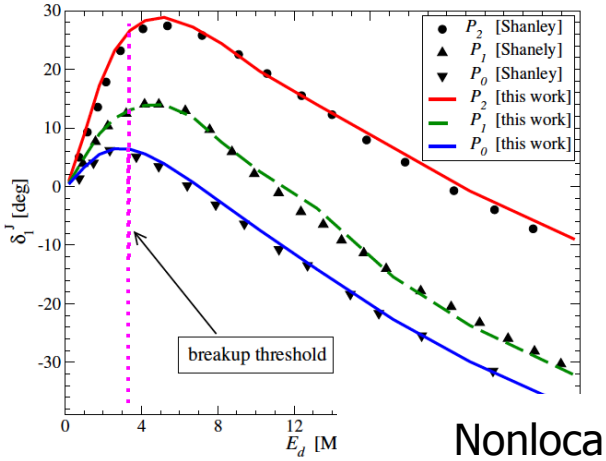

Microscopic optical potential (Rotureau, FN, et al)

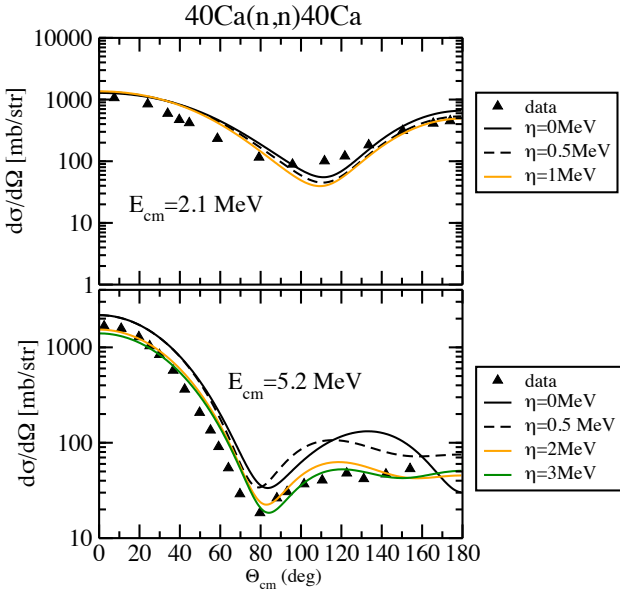

Nonlocal effects in (d,p) inclusive (Potel, Li, FN)

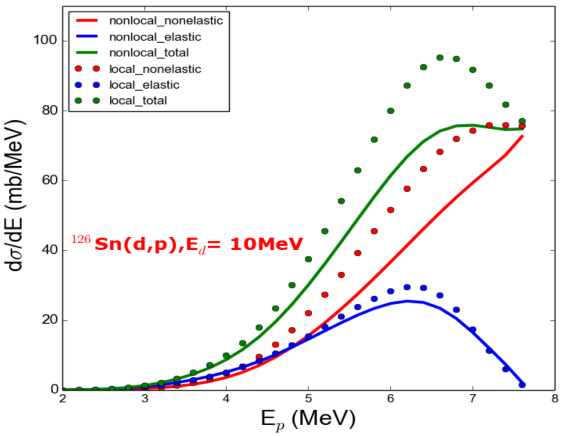

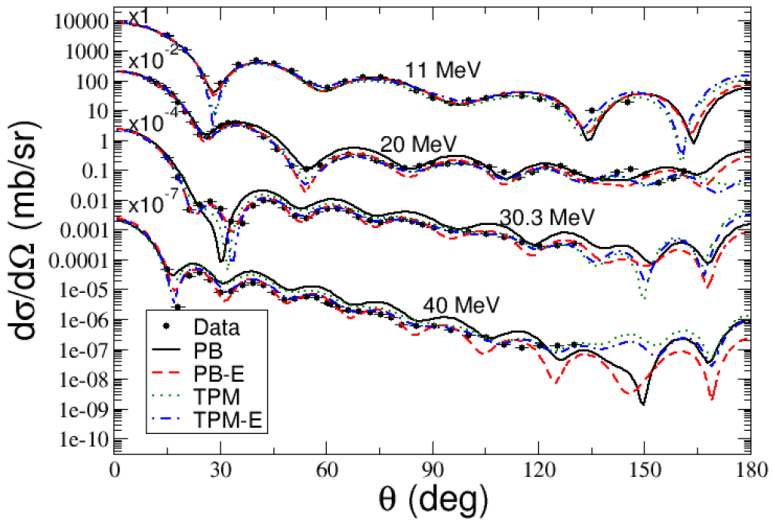

Non-local global nA and pA potential (Bacq, Capel, Jaghoub, Lovell, FN)

Charge-exchange (Poxon-Pearson, Potel, FN)